TRMM Observations of Polarization Difference in 85 GHz: Information about Hydrometeors and Rain Rate

C. Prabhakara[1], R. Iacovazzi, Jr.[2], and J.-M. Yoo[3]

[1]NASA/Goddard Space Flight Center

[2]Raytheon ITSS Corporation

[3]EWHA Womans University, Seoul, South Korea

Submitted to

Journal of the Meteorological Society of Japan

Corresponding Author Address

C. Prabhakara

NASA/Goddard Space Flight Center, Code 913

Greenbelt, Maryland 20771

Phone : 301-614-6193; Fax : 301-614-6307; E-mail : cuddapah@climate.gsfc.nasa.gov

Abstract

Observations made by the Precipitation Radar (PR) and the Microwave Imager (TMI) radiometer on board the Tropical Rainfall Measuring Mission (TRMM) satellite help us to show the significance of the 85 GHz polarization difference, PD85, measured by TMI. Rain type, convective or stratiform, deduced from the PR allows us to infer that PD85 is generally positive in stratiform rain clouds, while PD85 can be markedly negative in deep convective rain clouds. Furthermore, PD85 increases in a gross manner as stratiform rain rate increases. On the contrary, in a crude fashion PD85 decreases as convective rain rate increases. From the observations of TMI and PR, we find that PD85 is a weak indicator of rain rate. Utilizing information from existing polarimetric radar studies, we infer that negative values of PD85 are likely associated with vertically-oriented small oblate or wet hail that are found in deep convective updrafts.

1. Introduction

Observations made by polarimetric radars have shown that horizontally-oriented oblate hydrometeors - rain drops and dry and wet ice aggregates in stratiform rain clouds - tend to give positive Z_{DR}, where Z_{DR} represents the differential reflectivity measured between the vertical and horizontal polarization. On the other hand, for hydrometeors that have vertical orientation, such as oblate hail and wet hail in convective rain clouds, Z_{DR} is found to be negative (see for e.g., Bringi et al., 1986; Vivekanandan et al., 1996; and Hubbert et al., 1998). Although the polarimetric radar observations indicate the existence of such vertically-oriented particles, their existence has not been inferred from microwave radiometer data.

On board the Tropical Rainfall Measuring Mission (TRMM) satellite, the Precipitation Radar (PR) and the TRMM Microwave Imager (TMI) radiometer make nearly simultaneous measurements. The PR operates at a wavelength of about 14 GHz, and it does not have dual-polarization capability. However, based on the a) vertical profiles and b) horizontal uniformity of PR reflectivity, rain is classified as convective or stratiform (NASDA/NASA, 1999). This information about rain type can be useful in the interpretation of the TMI data. It may be noted that the TMI radiometer has Vertical- and Horizontal-polarization (V- and H-pol) channels near 10, 19, 37 and 85 GHz and a V-pol channel near 21 GHz. Also, the TMI has a conical-scan geometry with a 760 km wide swath of measurements, while the PR has a 220 km wide cross-track scan that is centered in the TMI swath.

In some radiative transfer theoretical modeling studies (see for e.g., Wu and Weinman, 1984; and Kummerow, 1987) the dependence of the brightness temperature difference $T_{V\text{-pol}}$ - $T_{H\text{-pol}}$ (PD) on rain rate was investigated for some channels of the passive microwave radiometers SMMR[1] and SSM/I[2]. Model calculations of Wu and Weinman showed that because of differences in scattering of V-pol and H-pol radiation by horizontally-oriented ice hydrometeors, the polarization difference in the 37 GHz region, PD37, is positive, and this PD37 increases with rain rate. Similar model calculations made for the 85 GHz microwave region by Kummerow showed no clear association between PD85 and rain rate. In these two studies, wet and dry hail are treated as horizontal oblates.

Heymsfield and Fulton (1994) found, with the help of land-based radar rain observations, that the polarization difference PD85 over stratiform rain regions given by the microwave radiometer SSM/I is positive and is generally less than 5 K. On the other hand, they indicate over convective rain areas PD85 is near zero. From these observations, they suggest that precipitation-sized ice particles in stratiform clouds that tend to be oriented horizontally as they fall through relatively weak vertical motions, such as snow or ice-aggregates, produce PD85 that is greater than zero. They also suggest that strong updrafts that are present in convective rain clouds could lead to tumbling of ice hydrometeors, which obliterates preferred orientation and hence PD85 is near zero.

In addition to the near zero or greater than zero PD85 observations, we notice in a few SSM/I observations that PD85 has small negative values (~ -1 K to -2 K). In

---

[1] Scanning Multichannel Microwave Radiometer: *Gloersen and Hardis (1978).*

[2] Special Sensor Microwave/Imager: *Radiometer of the Defense Meteorological Satellite Program (DMSP) that has 19, 37 and 85 GHz channels in dual polarization and a 22 GHz channel in vertical polarization. This radiometer observes the earth's surface and atmosphere in a conical scan with an incidence angle of ~ 50^0 (for more details see Hollinger et al., 1985).*

the past such negative values were disregarded. With the availability of TRMM satellite data, we have an extensive amount of microwave radiometer observations together with radar rain rates over the tropics. Now, we can probe the significance of negative PD85 with the help of this extensive set of TRMM observations, which have better spatial resolution than SSM/I. Also, in some rain retrieval methods PD85 is used as a parameter (see for e.g. Olson et al., 1999). The TRMM data can help us to evaluate the usefulness of PD85 as a parameter in rain retrievals.

2. TRMM Observations

In order to assess the relatively weak polarization effects induced by hydrometeors on microwave radiation, as a prerequisite we have to minimize the strong polarization effects that can be introduced by the earth's surface. Ocean and lake surfaces, as well as desert sand and soil moisture, can polarize microwave radiation. Generally, in a given channel of the TMI radiometer, when extinction due to hydrometeors in the atmosphere is strong, the contamination in the data introduced by surface effects is masked. Compared to lower frequency channels of the TMI, in the 85 GHz channel the surface is easily masked in the presence of optically thick rain clouds. This is because of strong extinction in the 85 GHz. Such optically thick conditions are obtained when we find there is a local minimum in the spatial distribution of the 85 GHz brightness temperature data ($T85h_{min}$).

It was shown in a rain retrieval study by Prabhakara et al. (2000 - hereafter PIWD), that the presence of a Cb can be inferred from a $T85h_{min}$. Furthermore, the mean value of the horizontal gradient of T85h, $\overline{dT85h/dr}$, around the $T85h_{min}$ helps to classify the Cb as convective or decaying type. Here, r is the radial distance from the center of the Cb. When $\overline{dT85h/dr} < 1\ Kkm^{-1}$, i.e., when T85h is nearly uniform horizontally, PIWD find from the PR measurements that on average the rain rate is weak and it is predominantly of stratiform type. This corresponds to the decay phase in the evolution of Cbs (Houze, 1997). In this study, for brevity we refer to decaying Cbs as stratiform Cbs. On the other hand, when $\overline{dT85h/dr} > 1$ Kkm^{-1}, i.e., when T85h is significantly non-uniform horizontally, on average the radar data show that the rain is largely of convective type, corresponding to vigorous Cbs. These characteristic of the horizontal distribution in T85h are illustated here with the aid of nearly simultaneous observations of Hurricane Floyd made by TRMM radar and radiometer.

The horizontal distribution of 85 GHz brightness temperature in the H-pol, T85h, measured by the TMI radiometer for Hurricane Floyd on September 13, 1999 as it approached the Bahama Islands in the Western Atlantic is shown in Figure 1a. Applying the above Cb identification method to the T85h observations of Hurricane Floyd, we show in Figure 1b the local minima that are produced as a result of strong scattering by ice hydrometeors. Based on TRMM Precipitation Radar (PR) rain rate estimates for the same region, shown in Figure 1c, we find these T85h minima correspond closely to PR rain centers or Cbs in different stages of their evolution. Based on earlier radar observational studies of MCSs (Houze, 1993), we assume the radius of these Cbs on the average is 10 km. The mean rain rate in each Cb is estimated from the "near-surface" PR rain rate (see TRMM 2A-25 Product in NASDA/NASA, 1999). The TRMM data associated with these $T85h_{min}$ can thus help us to explore, for both types of Cbs over land and ocean, the relationships a) between $T85h_{min}$ and the polarization difference PD85 induced by hydrometeors and b) between PD85 and PR measured rain rate.

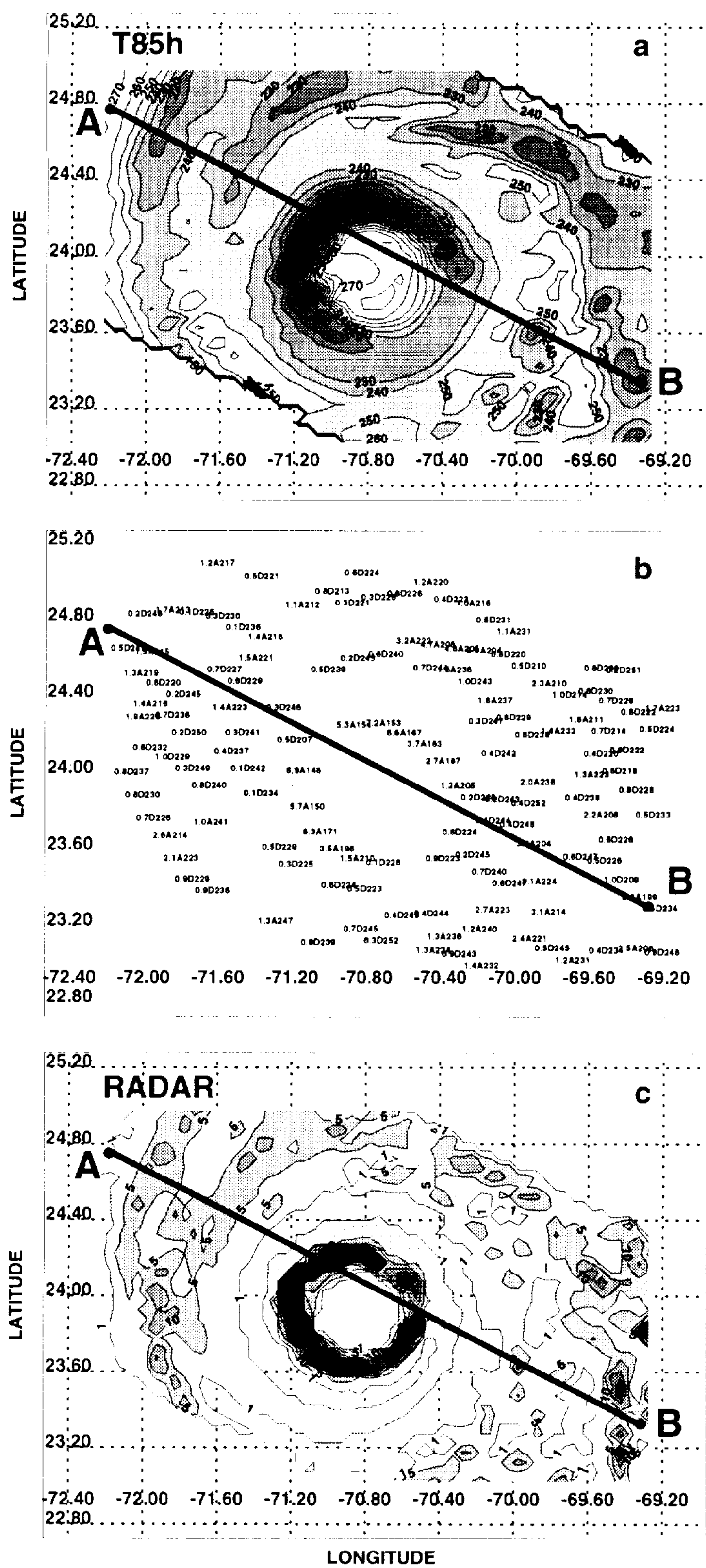

Figure 1: Hurricane Floyd on September 13, 1999 as it approached the Bahama Islands in the Western Atlantic Ocean: **a)** Map of T85h (K); **b)** Cbs inferred from T85h minima and dT85h/dr. In this map, each Cb is denoted by the magnitude of dT85h/dr (Kkm^{-1}) (Left), followed by the letter A or D (Center), and then the value of $T85h_{min}$ (K) (Right). The letters A and D indicate active growing Cbs and decaying Cbs, respectively.; **c)** PR rain rate ($mmhr^{-1}$). Note, the line AB denotes the cross section used in Figure 4.

In Figure 2a, a scatterplot of $T85h_{min}$ versus PD85 is shown for numerous Cbs deduced from 18 Mesoscale Convective Systems (MCSs) that occurred over different continental land regions covered by the TRMM satellite. For a given MCS, the date, time, location, total number of Cbs, and number of Cbs with negative polarization can be found in Table 1. From Figure 2a, we see a sector of densely-packed data points, and an adjacent sector where data points are not as densely packed. The significance of these two data configurations is brought to light by separating them into stratiform and convective types in the manner mentioned above with the help of the parameter $\overline{dT85h/dr}$. When this parameter has a value less than 1 Kkm^{-1}, we find the data are densely packed, as shown in Figure 2b. From PR observations, we discern that these data represent Cbs that are predominantly of stratiform type. The majority of the less-dense-packed data (see Figure 2c) correspond to convective Cbs that have been defined with $\overline{dT85h/dr} > 1$ Kkm^{-1}. A similar analysis performed over ocean (not presented here) shows results that are analogous to those found over land. It may be emphasized that the stratiform Cbs indicated in Figure 2b always have positive values of PD85. On the other hand, the convective Cbs, as indicated in Figure 2c, could have negative PD85 values. Note, in all the figures, an additional constraint requiring that $T85h_{min}$ must be less than 255 K is imposed to minimize surface contamination.

In Figures 3a and 3b, the relationship between PR derived rain rate and PD85 is shown for the data of Figures 2b and 2c, respectively. From Figure 3a, we note that for stratiform Cbs rain rate generally increases as PD85 increases, and PD85 is always greater than zero. On the other hand, from Figure 3b, we find convective rain rate increases in a gross fashion as PD85 decreases, and it can range from 10 K to -10 K. The correlation coefficient between rain rate and PD85 is weak, about 0.3 (see Figures

Table 1: The date, time, location, total number of Cbs, and number of Cbs with negative PD85 for each Land MCS

Month	Day	Time	Latitude	Longitude	# Minima	# Neg PD85
'99 Jan	19	1820	-18.13	28.76	39	2
'99 Feb	13	1431	-16.71	128.23	45	6
'99 Mar	3	311	-2.64	49.33	53	0
'98 May	26	1424	35.39	-92.31	48	5
'98 Jun	5	845	34.72	-88.39	69	3
'98 Jun	5	708	32.25	-92.48	23	2
'98 Jun	8	2010	12.75	-0.40	25	1
'98 Jun	9	1030	4.45	-65.43	63	0
'98 Jun	11	1347	32.42	155.56	43	0
'98 Jun	11	441	33.38	-98.92	40	6
'98 Jun	18	1500	26.99	116.30	37	2
'98 Jun	20	1411	26.64	114.81	21	2
'98 Jun	29	456	33.28	114.56	31	0
'98 Jul	5	223	23.76	81.28	45	0
'98 Jul	20	1648	28.09	116.51	22	1
'98 Sep	28	1838	31.33	-88.51	83	2
'99 Oct	17	618	18.25	84.09	32	1
'98 Dec	28	1034	-26.21	-58.31	72	1

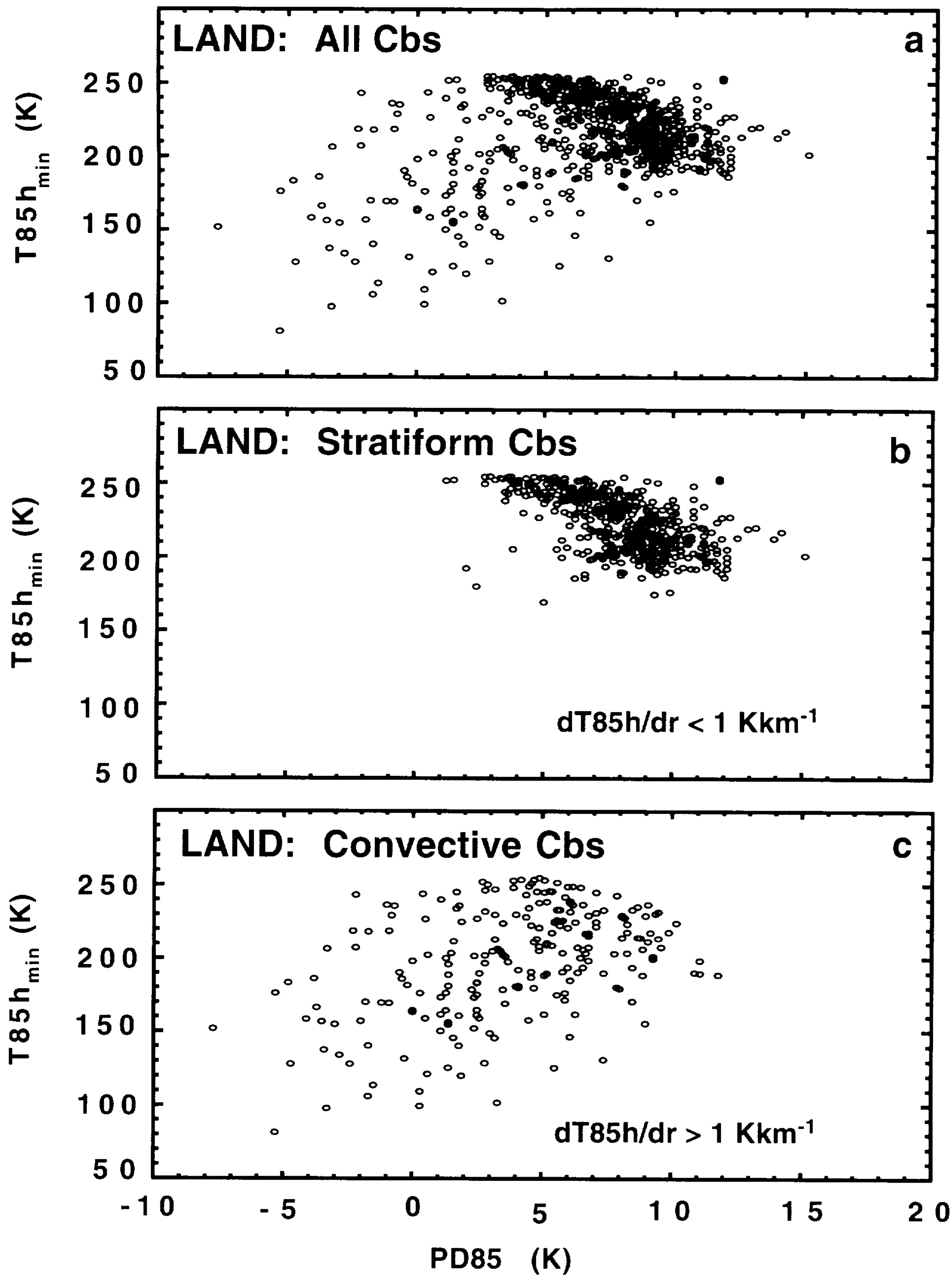

Figure 2: Based on TMI observations of eighteen Mesoscale Convective Systems over LAND -

a) Plot of $T85h_{min}$ (K) versus PD85 (K) for convective and stratiform Cbs (see text).

b) Plot of $T85h_{min}$ (K) versus PD85 (K) for stratiform Cbs ($dT85h/dr < 1\ Kkm^{-1}$).

c) Plot of $T85h_{min}$ (K) versus PD85 (K) for convective Cbs ($dT85h/dr > 1\ Kkm^{-1}$).

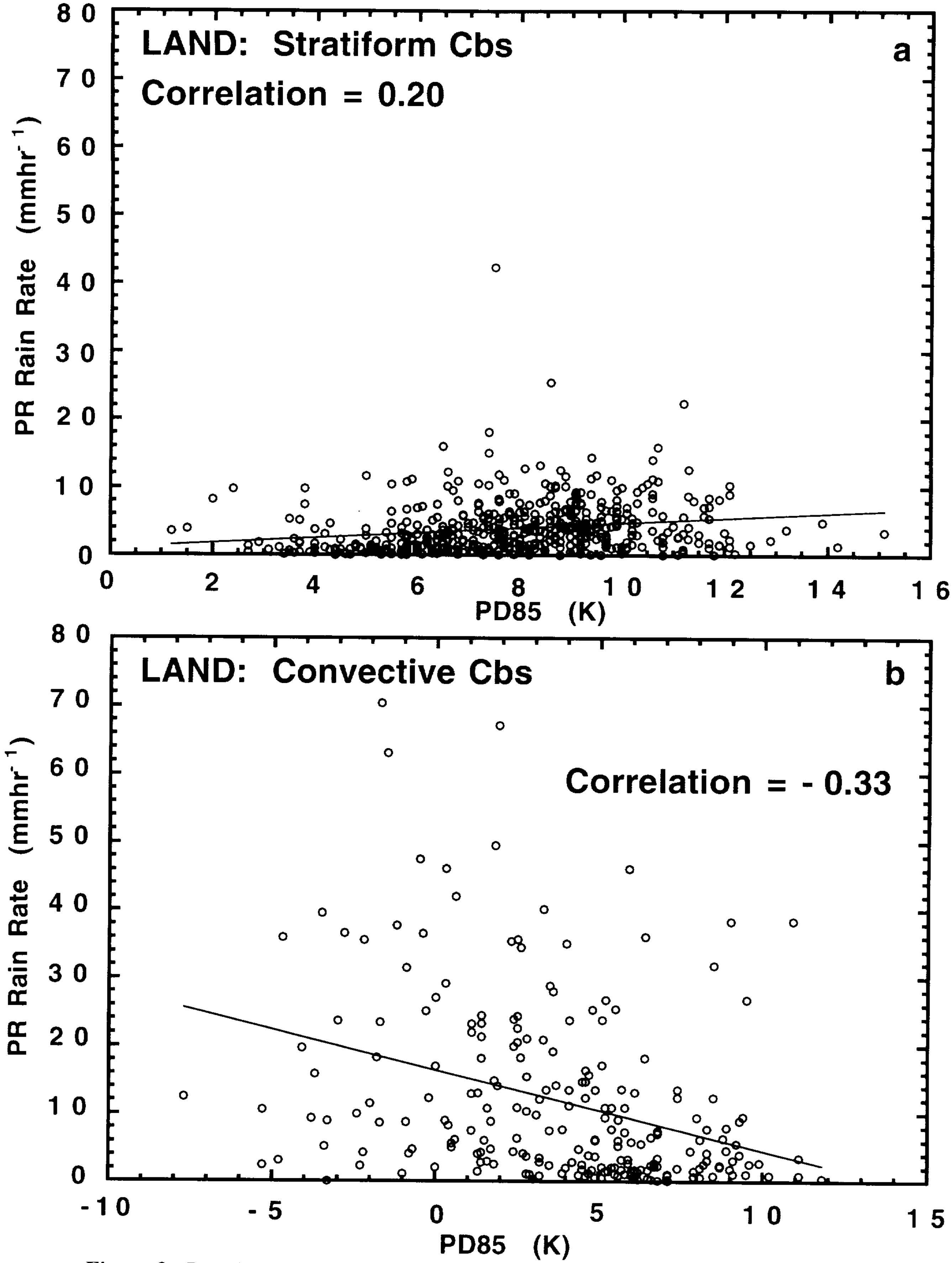

Figure 3: Based on TMI observations of eighteen Mesoscale Convective Systems over LAND -

a) Plot of PR near-surface rain rate ($mmhr^{-1}$) versus PD85 (K) for stratiform Cbs (see text).

b) Plot of PR near-surface rain rate ($mmhr^{-1}$) versus PD85 (K) for convective Cbs.

3a and 3b), and it has opposite sign for convective and stratiform rain. We find similar results for the rain events over ocean.

From the correlations between PR rain rate and PD85 presented above, we conclude that one cannot use PD85 as a robust parameter to estimate the rain rate. Such a parameter is used in a rain retrieval technique based on microwave radiometer data developed by Olson et al. (1999). The present study based on the radar observations shows the weakness of such parameterization.

The negative polarization shown in Figure 2c is explained with the help of cross sections of TMI brightness temperature, PR reflectivity, and PR near-surface rain rate data. We may note that the TMI and the PR data are not exactly coincident in space and time. For example, the scattering information of the 85 GHz channel that is highlighted here corresponds to the ice hydrometeors above the freezing level. On the other hand, close to the surface, the PR signal is directly from rain drops. Thus, the hydrometeors sensed in the 85 GHz do not necessarily represent the information pertaining to near-surface rain at a particular instant. Considering a mean fall velocity of rain drops of about 5 ms^{-1} over a distance of about 5 km, there will be a time lag of about 20 minutes between the hydrometeors above the freezing level and those at the surface. During this time interval, there can be differential advection between the near-surface layers of the atmosphere and the layers above the freezing level. Furthermore, evolution of ice hydrometeors over the period of 20 minutes can eclipse the link between near-surface rain drops and the hydrometeors aloft. For this reason, we do not expect that the details given by the TMI and the PR at a given instant are exactly relatable. In addition, the viewing geometry of the TMI and PR are different. Therefore, we can expect only a crude (~10 km) spatial agreement between these two sets of data.

We show in Figure 4a, a vertical cross section of the PR reflectivity data in the nadir direction along line $\overline{AB}$ of Figure 1. In Figure 4a, the location of the eye of Hurricane Floyd is indicated. Corresponding to the PR reflectivity data shown in Figure 4a, we present in Figures 4b, 4c, and 4d the PR near-surface rain rate, TMI H-pol brightness temperatures at 10, 19, 37, and 85 GHz, and PD85, respectively. Near-surface rain rate in Figure 4b on either side of the eye of the hurricane exceeds 50 $mmhr^{-1}$. This is indicated in that figure with arrows. From Figure 4d, we find a few local minima in PD85, which are also indicated by arrows. These minima correspond approximately to the narrow convective updrafts indicated by sharp reflectivity peaks in Figure 4a. In particular, one such peak that rises above 10 km into the atmosphere is associated with a negative PD85 of about -7 K. This strongly suggests that the deep penetrating vertical updrafts produce negative PD85. We note that such deep penetrating updrafts constitute only a small fraction of the Cbs in a given MCS events (see Table 1). From the polarimetric radar studies mentioned earlier, negative Z_{DR} are found to be present in intense convective rain areas where vertically-oriented small oblate hail or wet hail particles are present (Vivekanandan et al., 1996). Based on this information, we infer that negative PD85 observed in strong convective events is related to negative Z_{DR}.

3. Conclusions

In this study, we have explored, with the help of the PR observations, the properties of the TMI measured 85 GHz polarization difference, PD85, in active and decaying Cbs. As explained in Section 2, the active Cbs are characterized strongly by convective rain, while the decaying Cbs contain mainly stratiform rain.

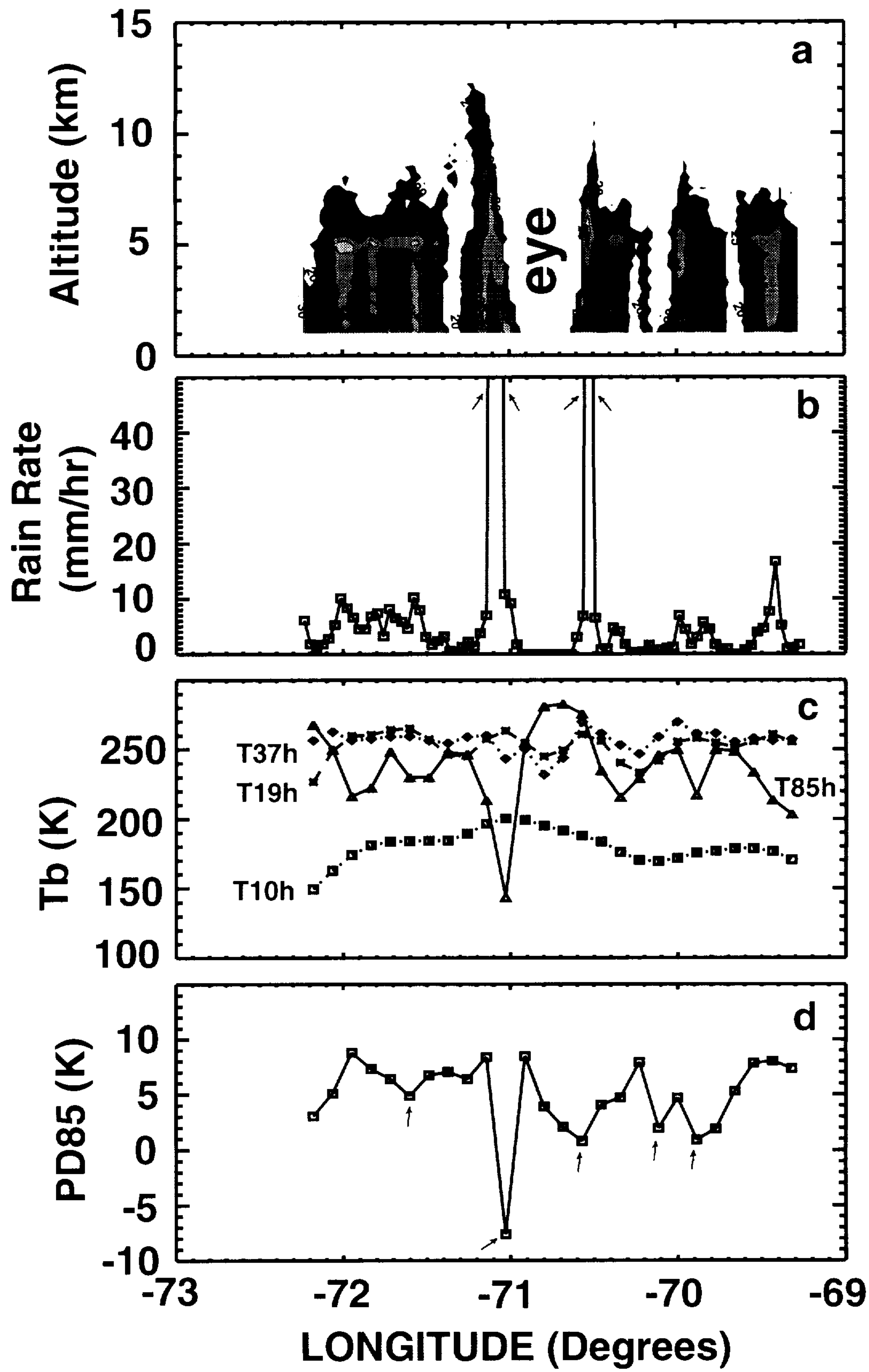

Figure 4: a) PR reflectivity as a function of height along line AB in Figure 1 for Hurricane Floyd on September 13, 1999 near the Bahama Islands. The hurricane eye is indicated.

b) PR near-surface rain rate ($mmhr^{-1}$) corresponding to Figure 4a.

c) TMI brightness temperature (K), Tb, in the H-pol channels corresponding to Figure 4a.

d) Polarization difference, PD85 (K), corresponding to Figure 4a.

In studies of MCSs using polarimetric radar differential reflectivity, Z_{DR}, observations (Bringi et al., 1986; Vivekanandan et al., 1996; and Hubbert et al., 1998), Z_{DR} is found to be positive in regions of horizontally-oriented melting ice aggregates. Such regions constitute stratiform rain areas of a MCS. From the PR and TMI data, we generally observe positive values of PD85 in regions dominated by stratiform rain. Association between positive values of PD85 and stratiform rain has been pointed out in previous studies that combined radar and micorwave radiometer data (see for e.g., Heymfield and Fulton, 1994).

In the polarimetric radar studies cited above, it was shown that vertically-oriented oblate hail or wet hail particles in convective precipitation shafts are responsible for negative values of Z_{DR}. The PR and TMI measurements indicate a new results that PD85 can be negative in convective Cbs. This leads us to indirectly infer that negative PD85 is linked to negative Z_{DR}. We may suggest that this inference is tentative and needs further study.

It was clarified in Section 2 that PD85 can explain only about 10 % of the variance contained in the stratiform and convective rain rates (see Figures 3a and 3b). In a study by Olson et al. (1999), it is hypothesized that PD85 can be used as a parameter in rain retrieval algorithms. From the observations of TMI and PR, we find that PD85 is not a robust parameter to retrieve rain.

Acknowledgments

We are thankful to the two anonymous reviewers of the paper, whose comments and suggestions have helped us to refine our manuscript. We thank Dr. James Weinman for many useful discussions and comments. We acknowledge the help given by the Distributed Data Archive Center of the Goddard Space Flight Center for providing the TRMM data.

References

Bringi, V. N., J. Vivekanandan, and J. D. Tuttle, 1986: Multiparameter radar measurements in Colorado convective storms. Part II: Hail detection studies. *J. Atmos. Sci.*, **43**, 2564-2577.

Gloersen P. and L. Hardis, 1978: Scanning multi-channel microwave radiometer (SMMR) experiment. In: Madris, C. R. (ed.) *Nimbus 7 User's Guide.* NASA/GSFC, Greenbelt, MD, 213-245 pp.

Heymsfield, G. M. and R. Fulton, 1994: Passive microwave and infrared structure of mesoscale convective systems. *Met. Atmos. Phys.*, **54**, 123-139.

Hollinger, J., R. C. Lo, G. Poe, R. Savage, and J. Pierce, 1987: *Special Sensor Microwave Imager Guide.* Naval Research Laboratory, Washington, D.C., 120 pp.

Houze Jr., R. A., 1997: Stratiform precipitation in regions of convection: A meteorological paradox? *Bull. Amer. Met. Soc.*, **78**, 2179-2196.

Hubbert, J., V. N. Bringi, L. D. Carey, and S. Bolen, 1998: CSU-CHILL polarimetric radar measurements from severe hail storms in Eastern Colorado. *J. Appl. Met.*, **37**, 749-775.

Kummerow, C. D. , 1987: Microwave radiances from horizontally finite, vertically structured precipitating clouds. Ph.D. Thesis, Univ. of Minnesota, Minneapolis, 146 pp.

NASDA/NASA, 1999: Tropical Rainfall Measuring Mission (TRMM) Precipitation Radar Algorithm Instruction Manual (Version 1.0). Available at

Olson, W. S., C. Kummerow, Y. Hong, and W.-K. Tao, 1999: Atmospheric latent heating distributions in the tropics derived from satellite passive microwave radiometer measurements. *J. Appl. Met*, **38**, 633-664.

Prabhakara C., R. Iacovazzi, Jr., J. A. Weinman, and G. Dalu, 2000: A TRMM microwave radiometer rain rate estimation method with convective and stratiform discrimination. *J. Met. Soc. Japan.*, **in press**.

Vivekanandan, J., R. Raghavan, and V. N. Bringi, 1996: Polarimetric radar modeling of mixtures of precipitation particles. *IEEE Trans. Geosci. Remote Sens.*, **31**, 1017-1030.

Wu, R. and J. A. Weinman, 1984: Microwave radiances from precipitating clouds containing aspherical ice, combined phase, and liquid hydrometeors. *J. Geophy. Res.*, **89**, 7170-7178.

Figure Captions

Figure 1: Hurricane Floyd on September 13, 1999 as it approached the Bahama Islands in the Western Atlantic Ocean:

a) Map of T85h (K)

b) Cbs inferred from T85h minima and $\overline{dT85h/dr}$. In this map, each Cb is denoted by the magnitude of $\overline{dT85h/dr}$ (Kkm^{-1}) (Left), followed by the letter A or D (Center), and then the value of $T85h_{min}$ (K) (Right). The letters A and D indicate active growing Cbs and decaying Cbs, respectively.

c) PR rain rate ($mmhr^{-1}$)

Note, the line $\overline{AB}$ denotes the vertical cross section used in Figure 4.

Figure 2: Based on TMI observations of 18 Mesoscale Convective Systems over LAND -

a) Plot of $T85h_{min}$ (K) versus PD85 (K) for all Cbs (see text).

b) Plot of $T85h_{min}$ (K) versus PD85 (K) for stratiform Cbs ($\overline{dT85h/dr} < 1$ Kkm^{-1}).

c) Plot of $T85h_{min}$ (K) versus PD85 (K) for convective Cbs ($\overline{dT85h/dr} > 1$ Kkm^{-1}).

Figure 3: Based on TMI observations of 18 Mesoscale Convective Systems over LAND -

a) Plot of PR rain rate ($mmhr^{-1}$) versus PD85 (K) for stratiform Cbs (see text).

b) Plot of PR rain rate ($mmhr^{-1}$) versus PD85 (K) for convective Cbs.

Figure 4: a) PR reflectivity as a function of height along line $\overline{AB}$ of Figure 1 for Hurricane Floyd on September 13, 1999 near the Bahama Islands. The hurricane eye has been indicated.

b) PR near-surface rain rate ($mmhr^{-1}$) corresponding to Figure 4a.

c) TMI brightness temperatures (K), Tb, in the H-pol channels corresponding to Figure 4a.

d) Polarization difference, PD85 (K), corresponding to Figure 4a.

Table 1: The date, time, location, total number of Cbs, and number of Cbs with negative PD85 for each Land MCS

Month	Day	Time	Latitude	Longitude	# Minima	# Neg PD85
'99 Jan	19	1820	-18.13	28.76	39	2
'99 Feb	13	1431	-16.71	128.23	45	6
'99 Mar	3	311	-2.64	49.33	53	0
'98 May	26	1424	35.39	-92.31	48	5
'98 Jun	5	845	34.72	-88.39	69	3
'98 Jun	5	708	32.25	-92.48	23	2
'98 Jun	8	2010	12.75	-0.40	25	1
'98 Jun	9	1030	4.45	-65.43	63	0
'98 Jun	11	1347	32.42	155.56	43	0
'98 Jun	11	441	33.38	-98.92	40	6
'98 Jun	18	1500	26.99	116.30	37	2
'98 Jun	20	1411	26.64	114.81	21	2
'98 Jun	29	456	33.28	114.56	31	0
'98 Jul	5	223	23.76	81.28	45	0
'98 Jul	20	1648	28.09	116.51	22	1
'98 Sep	28	1838	31.33	-88.51	83	2
'99 Oct	17	618	18.25	84.09	32	1
'98 Dec	28	1034	-26.21	-58.31	72	1

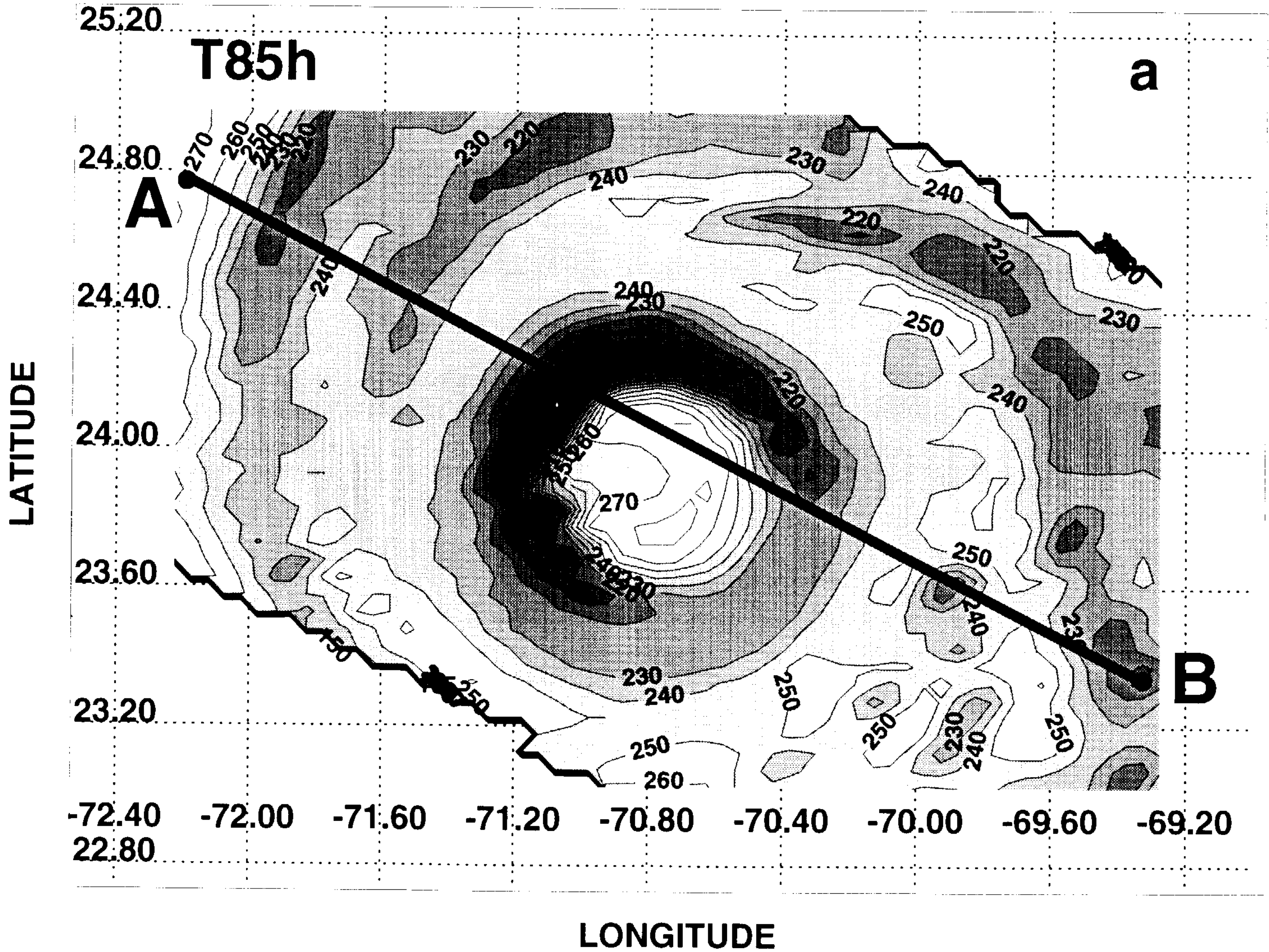
T85h
a
A
B
LATITUDE
LONGITUDE
25.20
24.80
24.40
24.00
23.60
23.20
22.80
-72.40
-72.00
-71.60
-71.20
-70.80
-70.40
-70.00
-69.60
-69.20
270
260
250
240
230
220

Fig. 1a

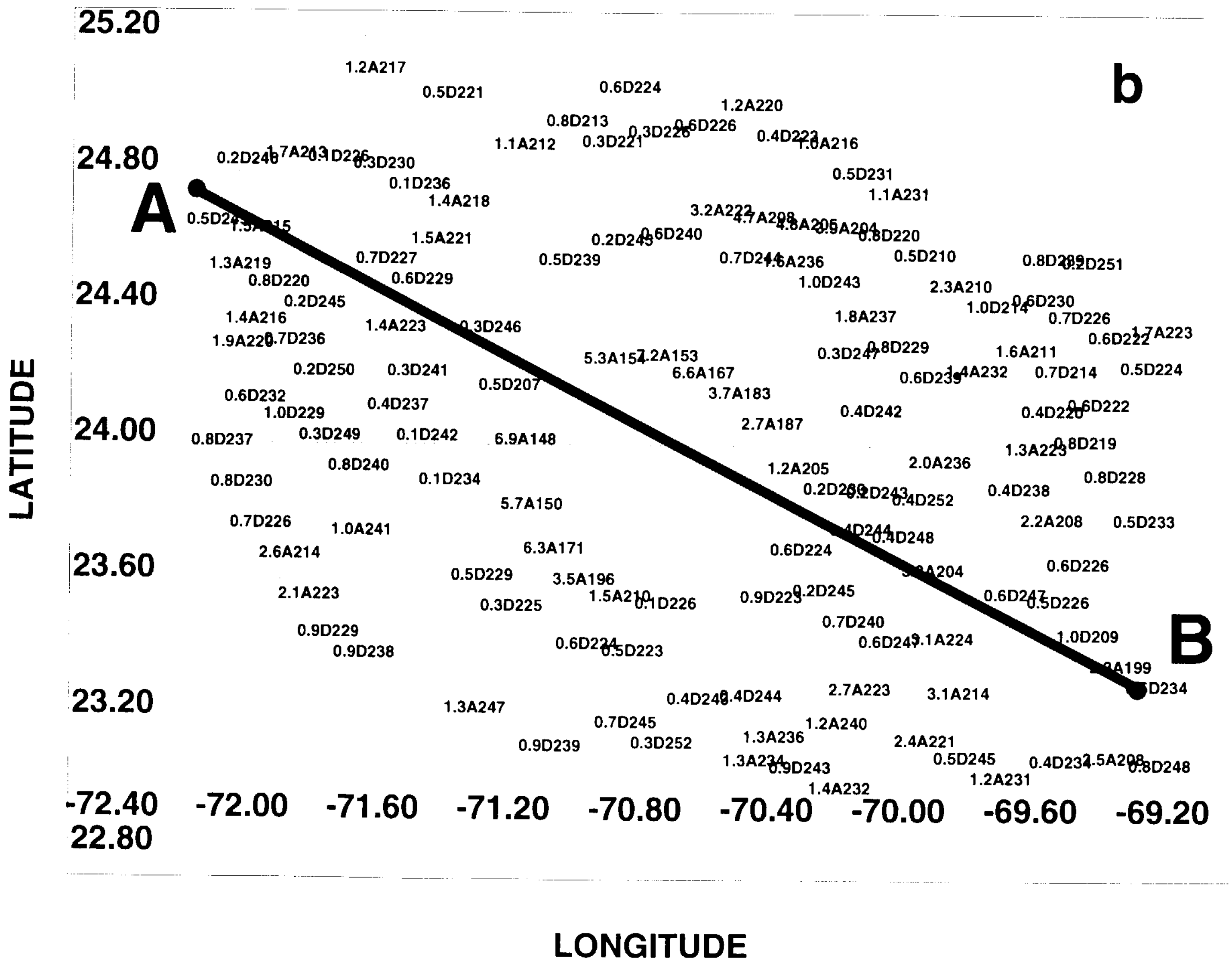

LATITUDE
LONGITUDE
25.20
24.80
24.40
24.00
23.60
23.20
22.80
-72.40
-72.00
-71.60
-71.20
-70.80
-70.40
-70.00
-69.60
-69.20
A
B
b
1.2A217
0.5D221
0.6D224
1.2A220
0.8D213
1.1A212
0.3D221
0.5D231
1.1A231
0.3D230
0.1D236
1.4A218
1.5A221
0.5D239
0.8D220
0.5D210
1.3A219
0.7D227
0.6D229
1.0D243
2.3A210
0.2D245
1.4A216
1.4A223
1.8A237
0.6D230
0.7D226
0.2D250
0.3D241
0.5D207
6.6A167
1.6A211
0.7D214
0.5D224
0.6D232
1.0D229
0.4D237
3.7A183
0.4D242
0.8D237
0.3D249
0.1D242
6.9A148
2.7A187
0.8D240
0.8D230
0.1D234
1.2A205
2.0A236
0.8D228
0.4D238
5.7A150
0.7D226
1.0A241
2.2A208
0.5D233
2.6A214
6.3A171
0.6D224
0.6D226
0.5D229
3.5A196
2.1A223
0.3D225
0.5D226
0.7D240
0.9D229
0.9D238
1.0D209
1.3A247
2.7A223
3.1A214
0.7D245
1.2A240
0.9D239
0.3D252
1.3A236
2.4A221
0.5D245
1.2A231
1.4A232

Fig. 1b

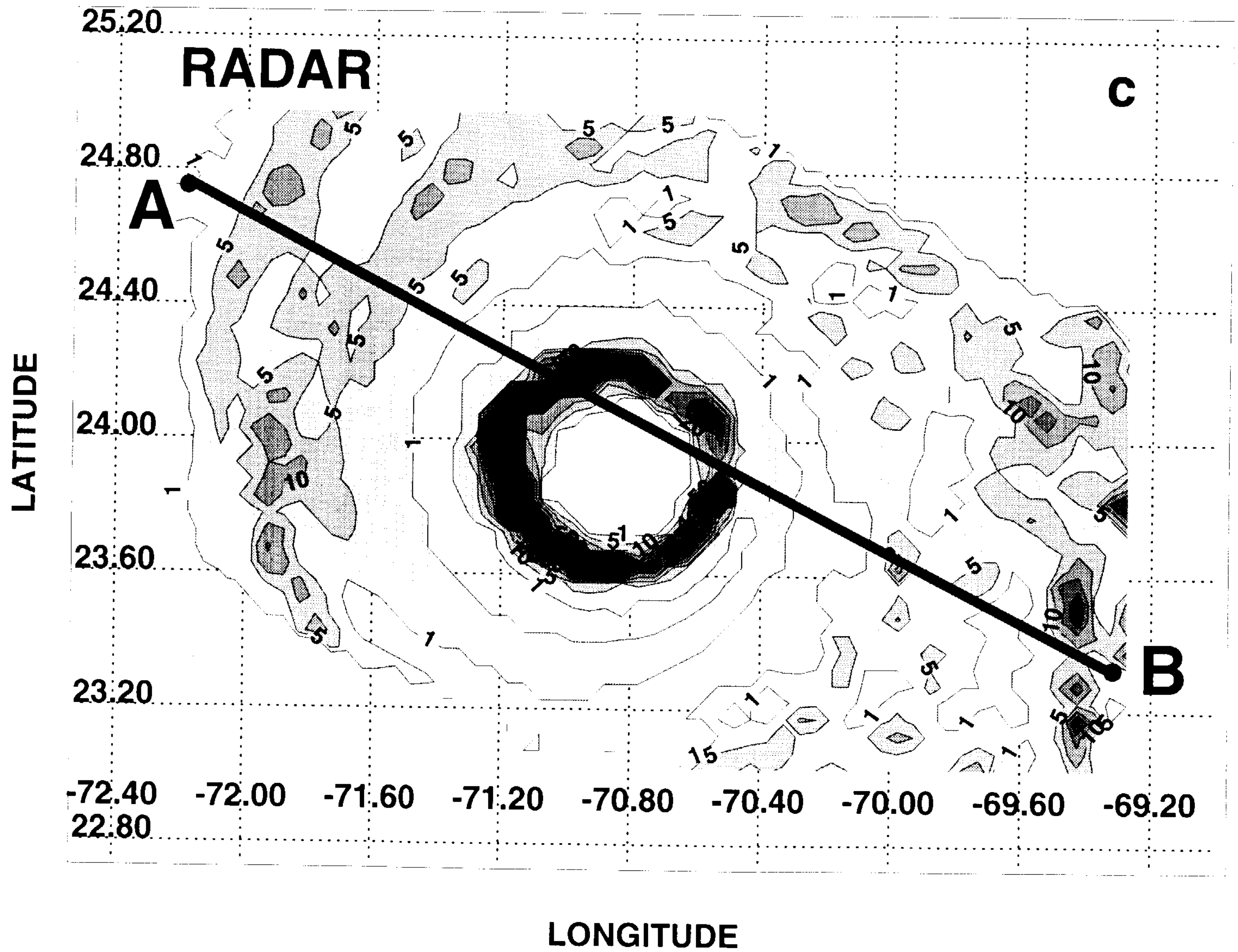
RADAR
c
A
B
25.20
24.80
24.40
24.00
23.60
23.20
22.80
-72.40
-72.00
-71.60
-71.20
-70.80
-70.40
-70.00
-69.60
-69.20
LATITUDE
LONGITUDE

Fig. 1c

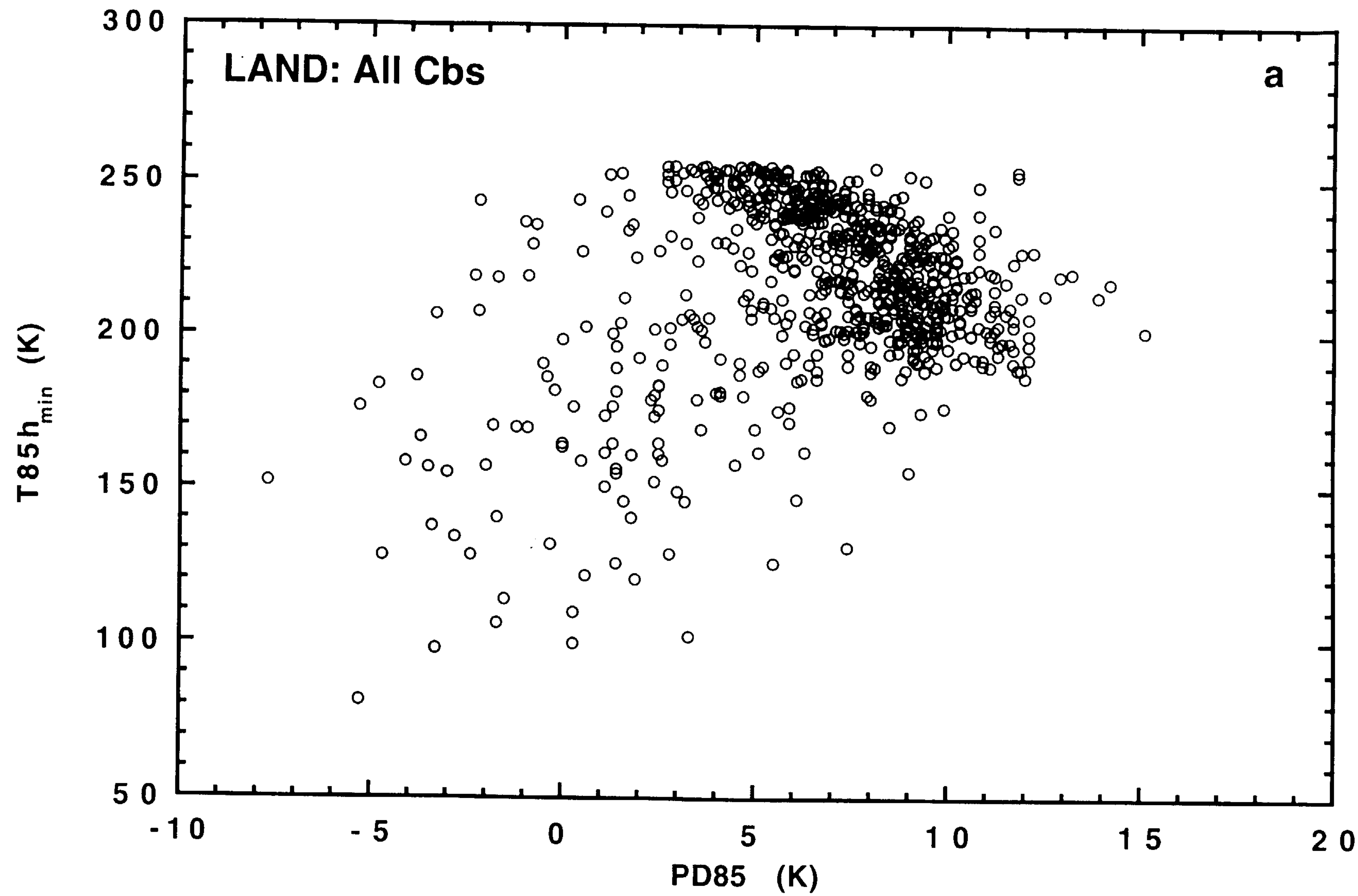

LAND: All Cbs
a
300
250
200
150
100
50
-10
-5
0
5
10
15
20
PD85 (K)
T85h_min (K)

FIG. 2a

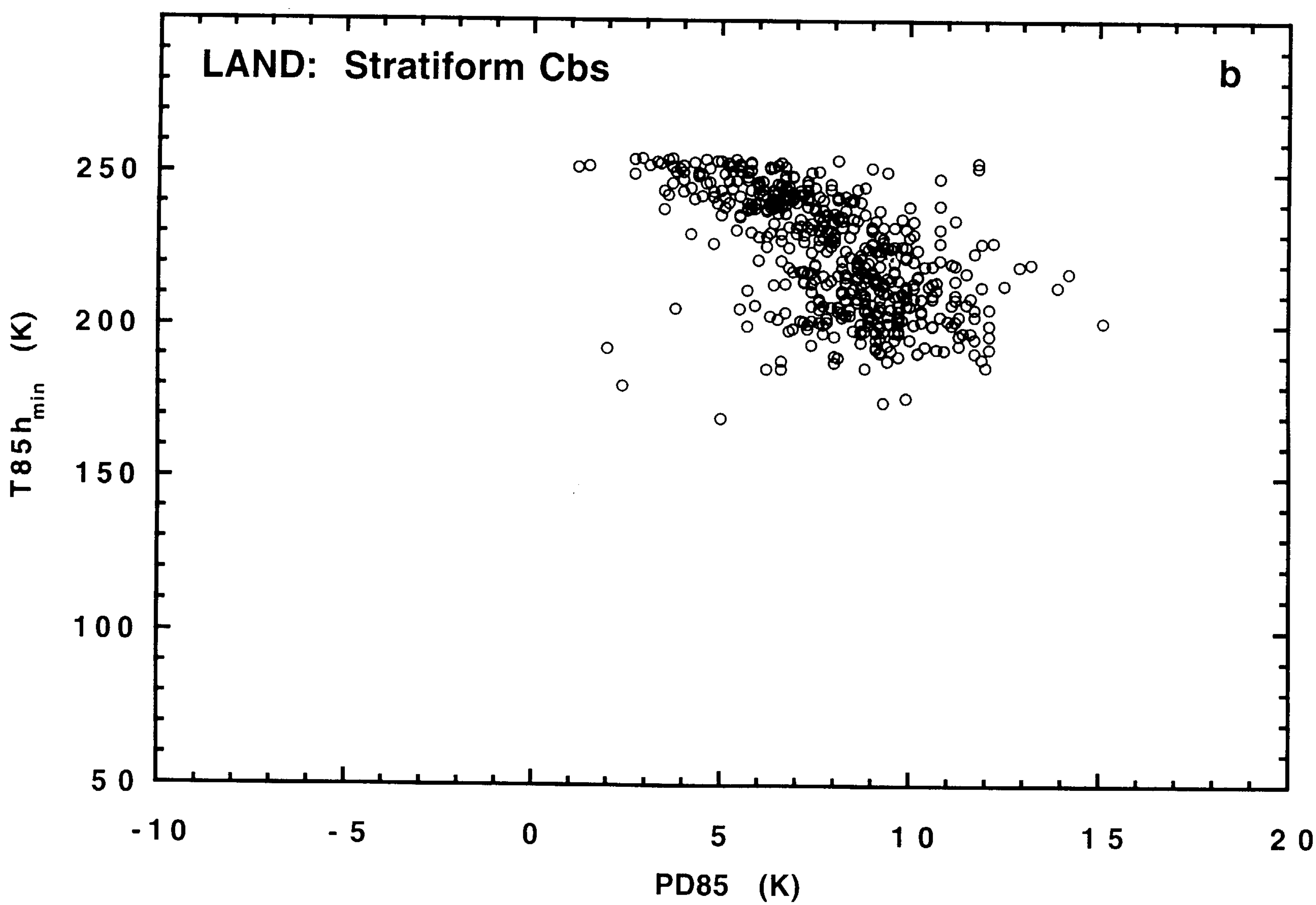

LAND: Stratiform Cbs
b
250
200
150
100
50
T85h min (K)
-10
-5
0
5
10
15
20
PD85 (K)

Fig. 2b

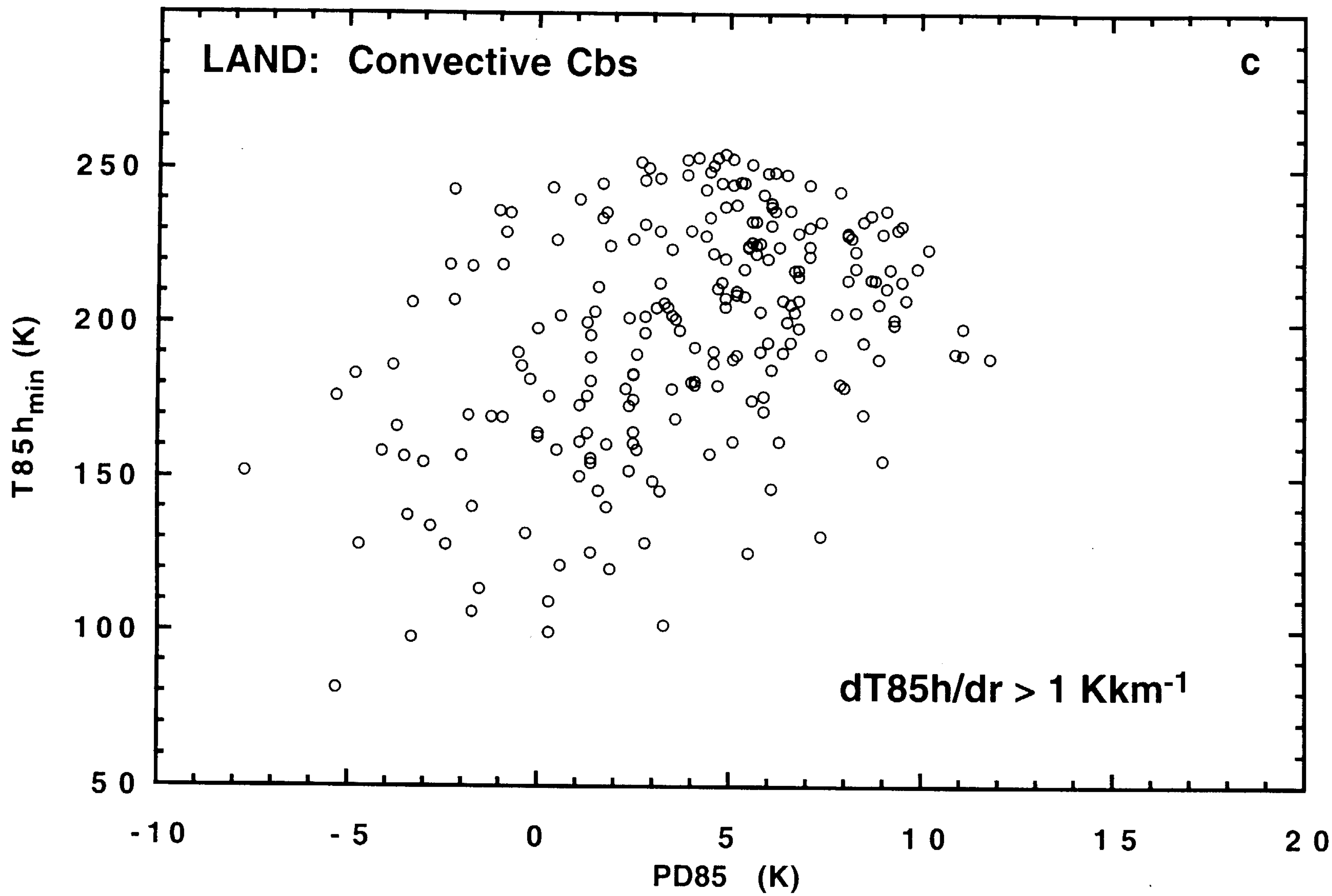
LAND: Convective Cbs
c
dT85h/dr > 1 Kkm-1
T85h_min (K)
250
200
150
100
50
-10
-5
0
5
10
15
20
PD85 (K)

Fig. 2c

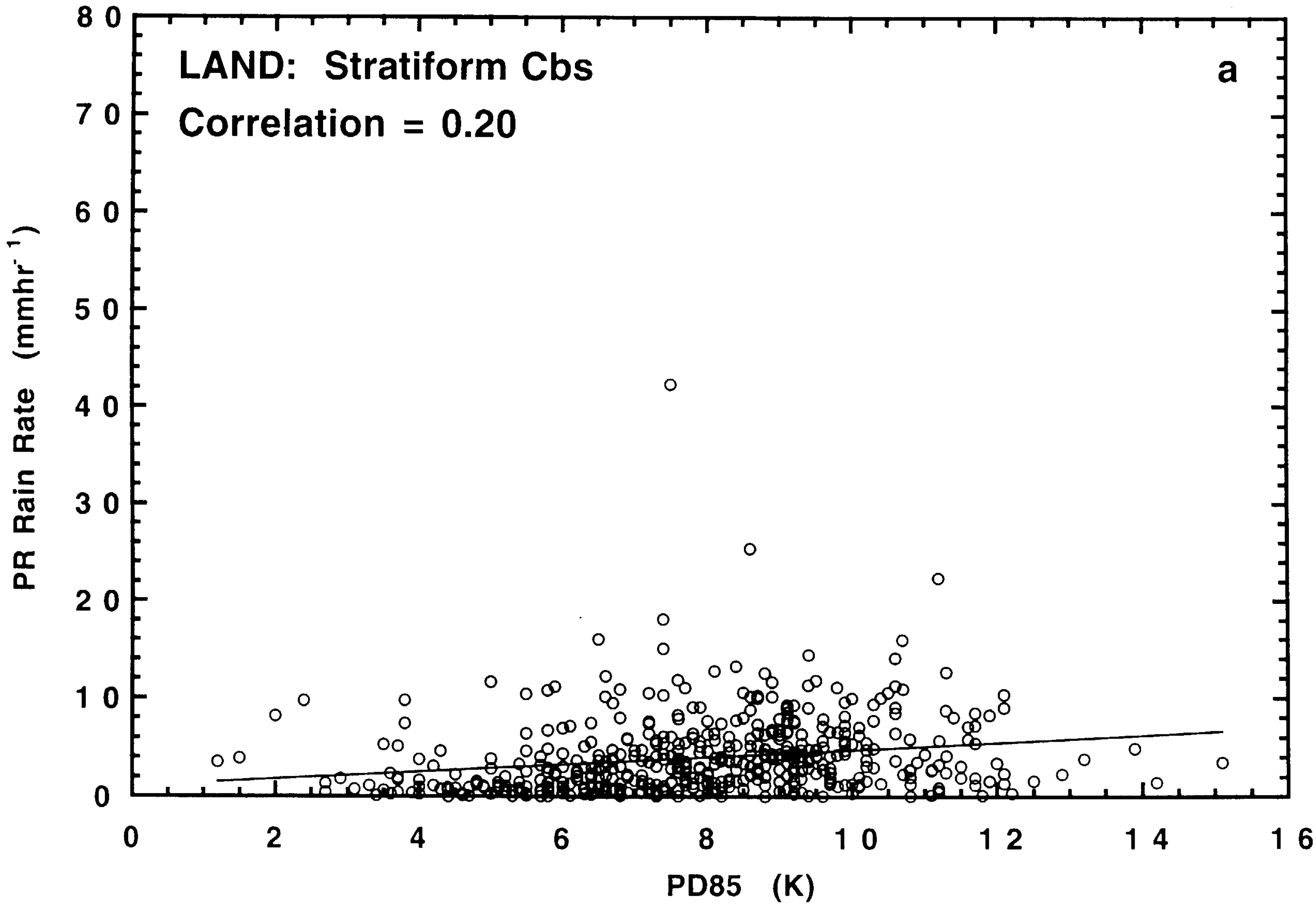
LAND: Stratiform Cbs
Correlation = 0.20
a
PR Rain Rate (mmhr-1)
PD85 (K)
0
2
4
6
8
10
12
14
16
20
30
40
50
60
70
80

Fig. 3a

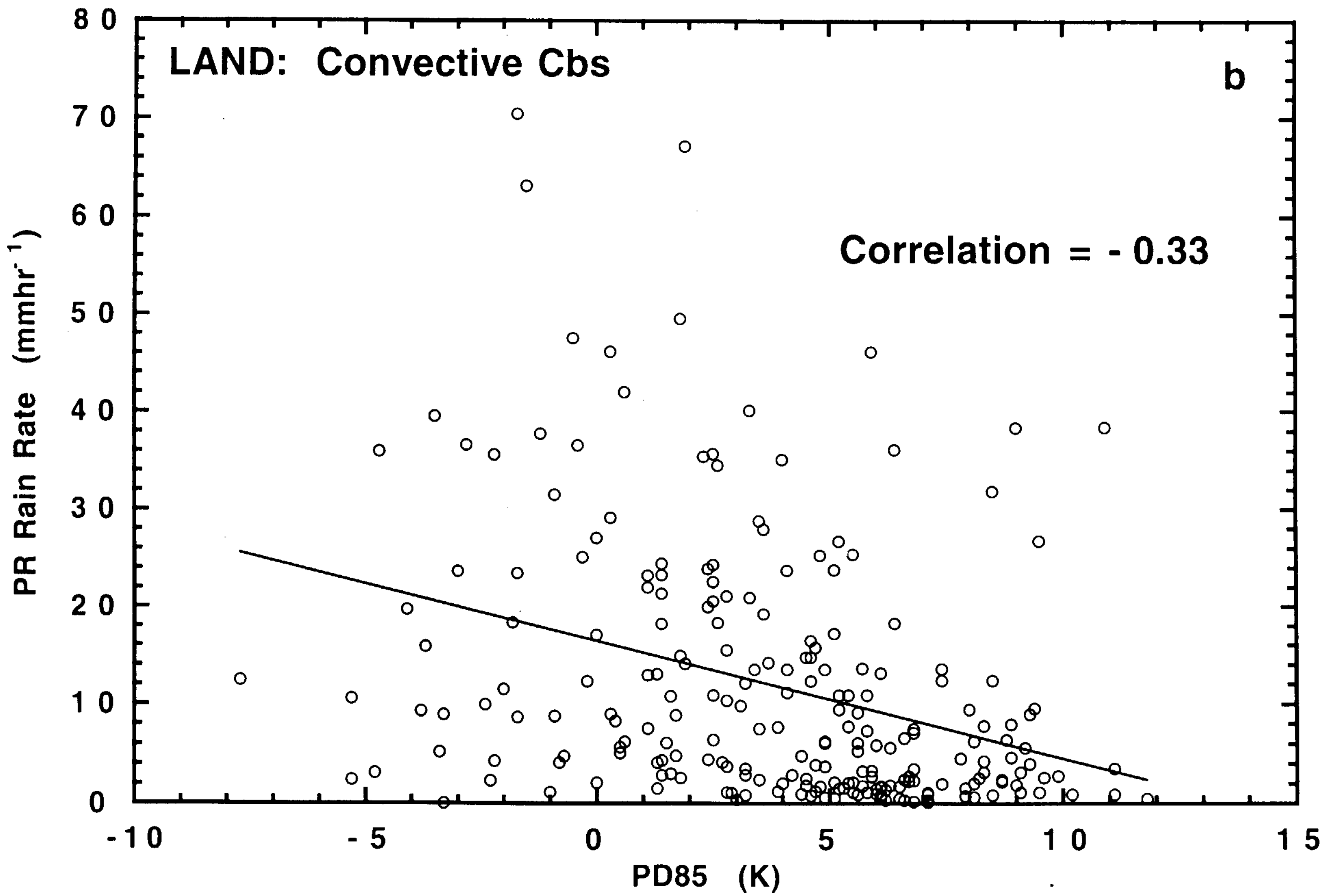

LAND: Convective Cbs
b
Correlation = - 0.33
PR Rain Rate (mmhr⁻¹)
80
70
60
50
40
30
20
10
0
-10
-5
0
5
10
15
PD85 (K)

Fig. 3b

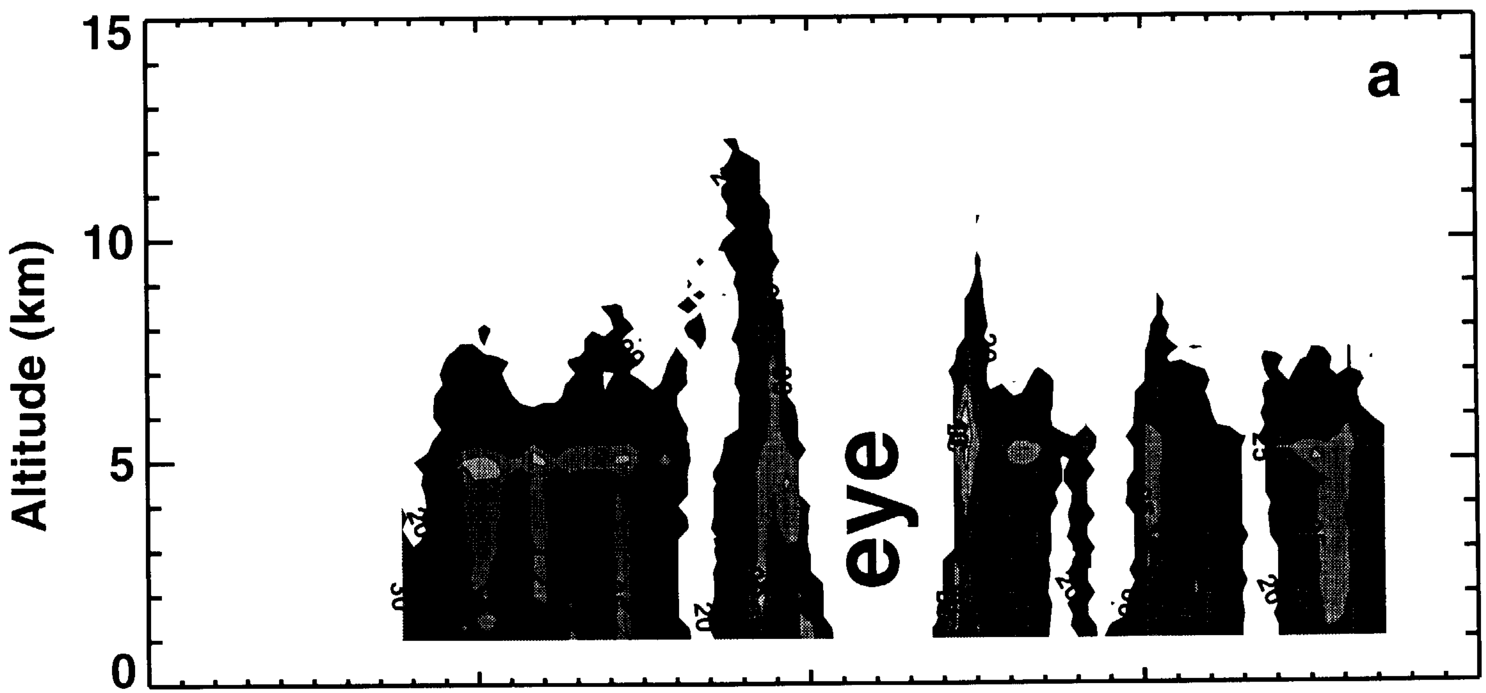

Fig. 4a

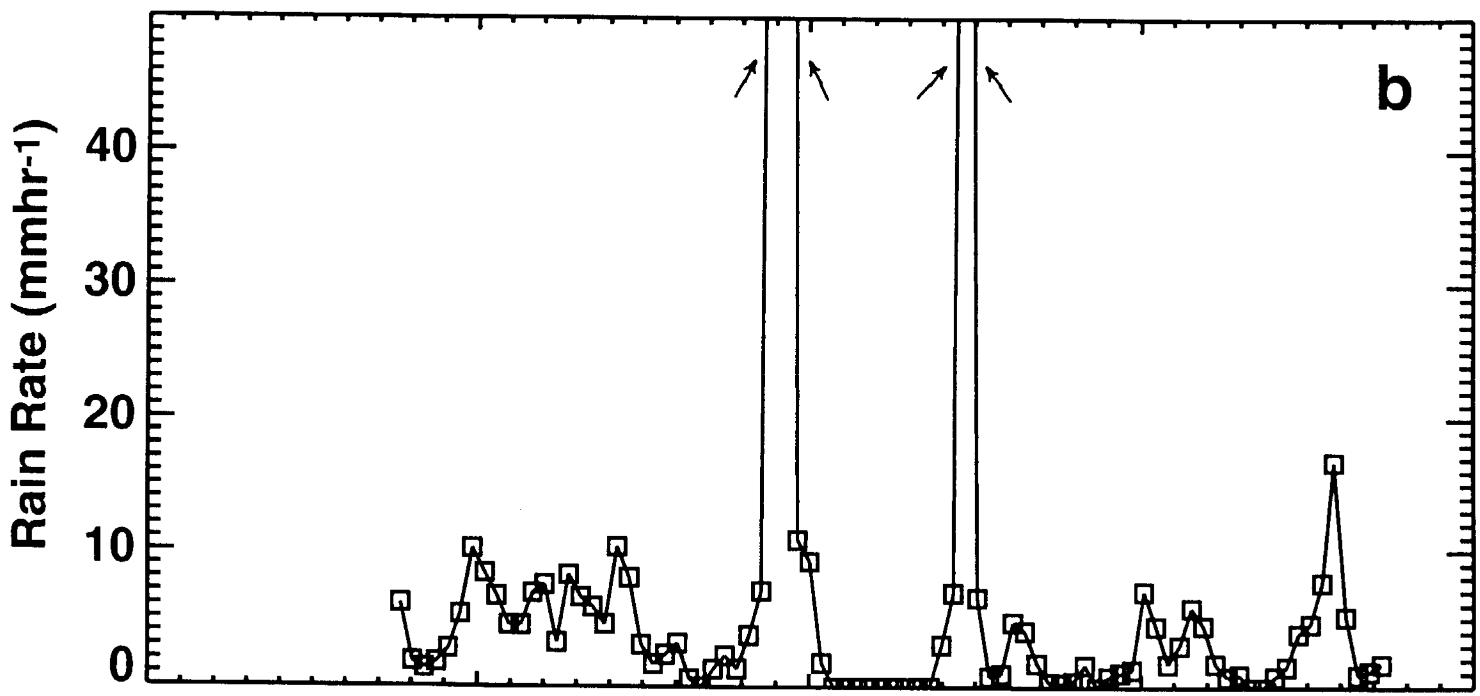

Fig. 4b

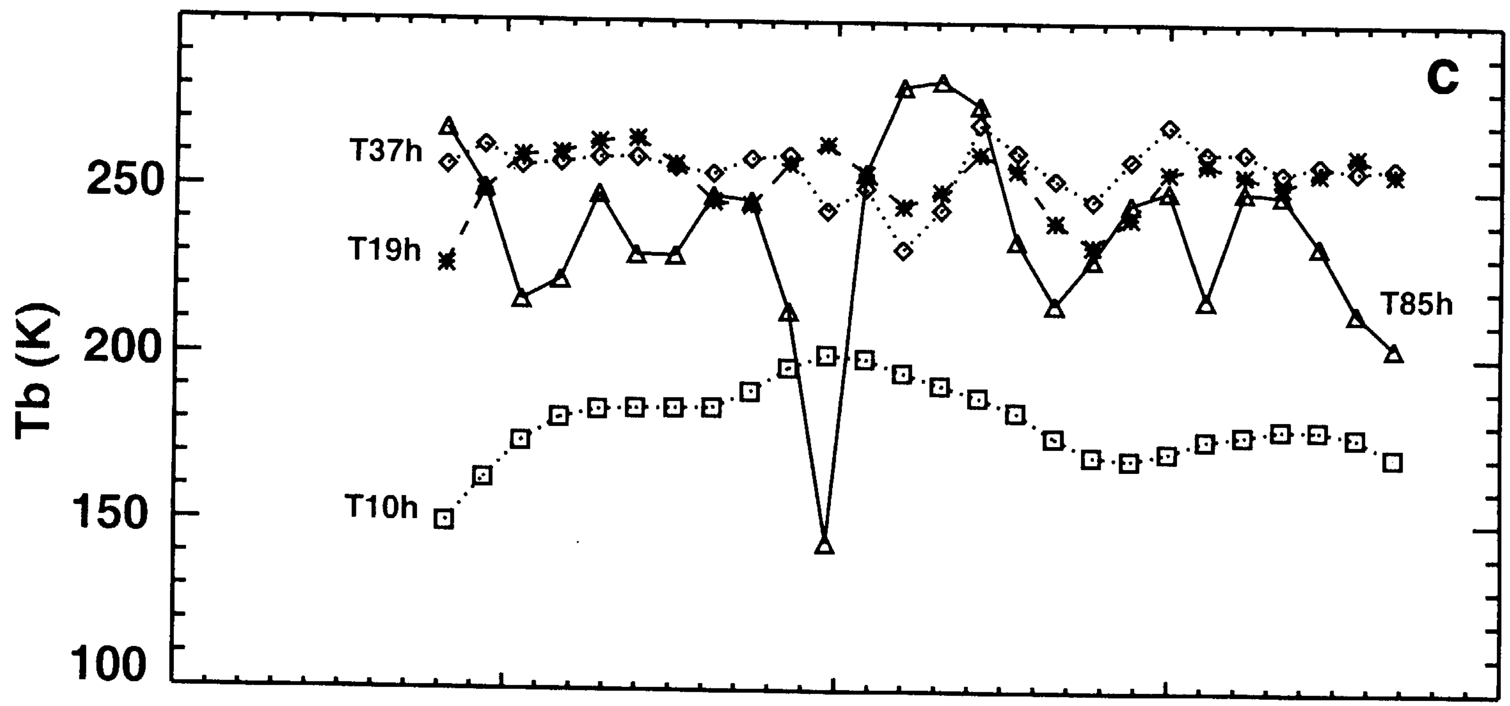

Fig. 4c

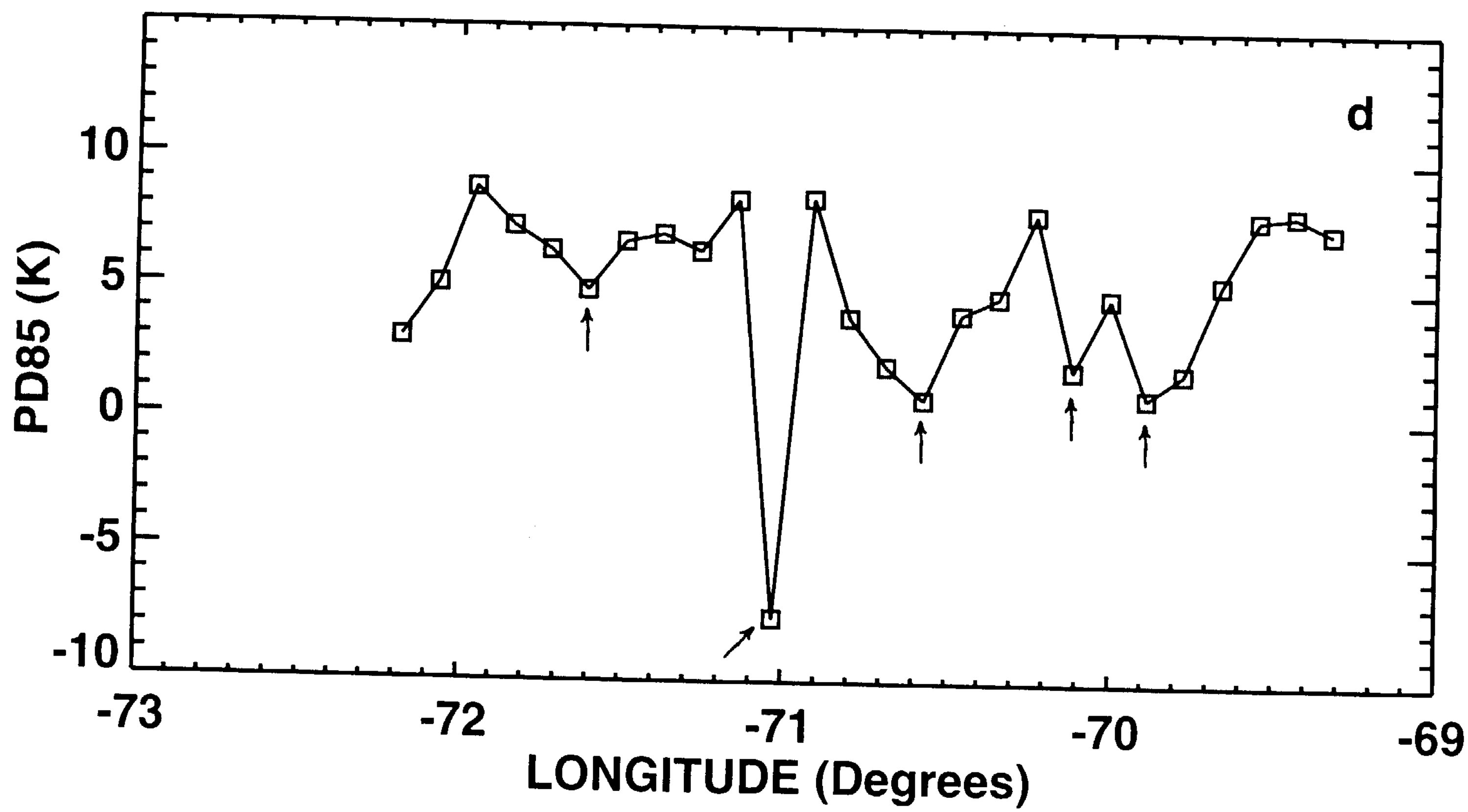

Fig. 4d